Simulating three phase induction motor performance during different voltage sag types

Elgenedy, M. A.; Moussa, A.; Negm, E.

Published in:
2012 15th International Middle East Power System Conference (MEPCON)

Publication date:
2012

Document Version
Author accepted manuscript

Simulating three phase induction motor performance during different voltage sag types

Elgenedy, M. A.; Moussa, A.; Negm, E.

Published in:
2012 15th International Middle East Power System Conference (MEPCON)

Publication date:
2012

Document Version
Early version, also known as pre-print

Simulating Three Phase Induction Motor Performance During Different Voltage Sag Types

M. A. Elgenedy
Electrical Engineering Department,
Alexandria University, Egypt
m.atef.elgenedy@gmail.com

A. Moussa
Pharos University
Alexandria, Egypt
Aymousa1@yahoo.com

E. Negm
Electrical Engineering Department,
Alexandria University, Egypt
emtethal_1934@yahoo.com

***Abstract*—This paper provides a detailed assessment of the performance of different induction motor sizes when subjected to different voltage sag types of different characterizations. To achieve such goal, a transient induction motor (IM) model was built using MATLAB/SIMULINK package, another model was built which is the voltage sag generator that provides the ability of generating almost any sag type with any customized characterizations.**

***Keywords*— Induction motors (IMs), power quality (PQ), symmetrical and unsymmetrical voltage sags, voltage sag characterizations.**

I. INTRODUCTION

Voltage sags are currently a matter of great interest because they can pose a number of problems in the supplied equipment depending on their particular sensitivity. Voltage sags can be either symmetrical or unsymmetrical, depending on the causes. If the individual phase voltages are equal and the phase relationship is 120º, the sag is symmetrical. Otherwise, the sag is unsymmetrical [1,2].

A three-phase short circuit or a large motor starting can produce symmetrical sags. Single line-to-ground, phase-to-phase, or two phase-to-ground faults due to lightning, animals, accidents, and other causes, as well as energizing of large transformers can cause unsymmetrical sags. Load and transformer connections can modify the type of sag experienced by a load [3,4]. The consequences of a voltage sag on the induction machine behaviour are speed loss and current and torque peaks that appear in the fault and recovery voltage instants. These transient effects can trigger the motor or system protection [1,2].

Section II shows the voltage sags classification and modeling, while Section III presents the induction motor model, then the sags consequences are analyzed in Sections IV and V.

II. MODELING A VOLTAGE SAG GENERATOR

Voltage sags experienced by three phase loads can be classified into seven types, denoted as A, B, C, D, E, F, and G.

Fig. 1 shows their phasor diagrams and table I includes their expressions [2], [5], where h is the sag magnitude ($0 \leq h \leq 1$), and in this paper, sag magnitude is the net root mean square voltage in percentage or per unit of system rated voltage. Sag type A is symmetrical, whereas types B to G are unsymmetrical.

Since the initial point-on-wave ψ_i affects the current and torque of the induction motor, the sag generator model should be able to handle it, thus if phase 'a' voltage is

$$v_a(t) = \sqrt{2}\ V\ \cos(\omega t + \alpha) \tag{1}$$

Let the initial instant t_i or fault instant is the instant when the sag begins, hence the initial point-on-wave ψ_i at the initial instant t_i is

$$\psi_i = \omega t_i + \alpha \tag{2}$$

If the sag begins at the initial instant t_i = 0 s, the angle of the 'a' phase voltage α matches up with the initial point-on-wave, hence $\psi_i = \alpha$. In all of the examples of this paper, sags begin at the initial instant t_i = 0 s, which gives $\psi_i = \alpha$.

The implemented sag generator model in this paper will generate voltage sags which are rectangular, they are univocally defined by their magnitude, their duration, and their initial point-on-wave. Fig. 2 and Fig. 3 show a part of the Simulink model for the voltage sag generator.

III. INDUCTION MOTOR MODEL

Studying the influence of voltage sags on the three phase induction motors requires modeling the induction motor in the transient state, so that the stator and rotor voltage equations, flux linkage equations and the torque equation referred to the *qd0* stationary reference frame are written in terms of the flux linkage per second ψ, and reactance x, instead of λ and L, where ($\psi = 2\pi f_{rated}\, \lambda$) and ($x = 2\pi f_{rated}\, L$). The operator p is used where ($p = d/dt$), ω_b is the synchronous speed at rated frequency where ($\omega_b = 2\pi f_{rated}$), ω_{re} is rotor speed in electrical radians [6-8].

(*N.B. the prime here denotes that the value is referred to the stator side*).

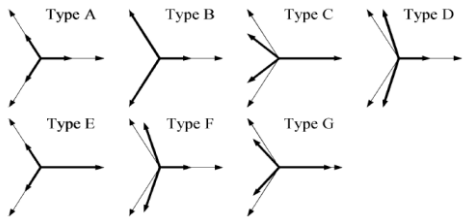

Fig. 1. Voltage sag types, all sags have $h = 0.5$.

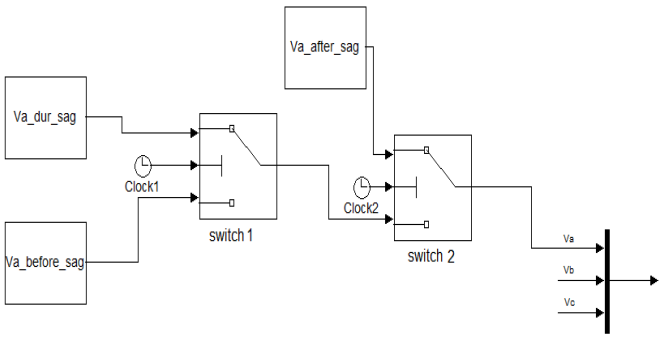

Fig. 2. Voltage sag generator phase 'a' Smulink model.

TABLE I
SAG TYPES IN EQUATION FORM.

Type A	Type B
$\underline{V}_a = hV$	$\underline{V}_a = hV$
$\underline{V}_b = -\frac{1}{2}hV - j\frac{\sqrt{3}}{2}hV$	$\underline{V}_b = -\frac{1}{2}V - j\frac{\sqrt{3}}{2}V$
$\underline{V}_c = -\frac{1}{2}hV + j\frac{\sqrt{3}}{2}hV$	$\underline{V}_c = -\frac{1}{2}V + j\frac{\sqrt{3}}{2}V$
Type C	**Type D**
$\underline{V}_a = V$	$\underline{V}_a = hV$
$\underline{V}_b = -\frac{1}{2}V - j\frac{\sqrt{3}}{2}hV$	$\underline{V}_b = -\frac{1}{2}hV - j\frac{\sqrt{3}}{2}V$
$\underline{V}_c = -\frac{1}{2}V + j\frac{\sqrt{3}}{2}hV$	$\underline{V}_c = -\frac{1}{2}hV + j\frac{\sqrt{3}}{2}V$
Type E	**Type F**
$\underline{V}_a = V$	$\underline{V}_a = hV$
$\underline{V}_b = -\frac{1}{2}hV - j\frac{\sqrt{3}}{2}hV$	$\underline{V}_b = -\frac{1}{2}hV - j\frac{1}{\sqrt{12}}(2+h)V$
$\underline{V}_c = -\frac{1}{2}hV + j\frac{\sqrt{3}}{2}hV$	$\underline{V}_c = -\frac{1}{2}hV + j\frac{1}{\sqrt{12}}(2+h)V$
Type G	
$\underline{V}_a = \frac{1}{3}(2+h)V$	
$\underline{V}_b = -\frac{1}{6}(2+h)V - j\frac{\sqrt{3}}{2}hV$	
$\underline{V}_c = -\frac{1}{6}(2+h)V + j\frac{\sqrt{3}}{2}hV$	

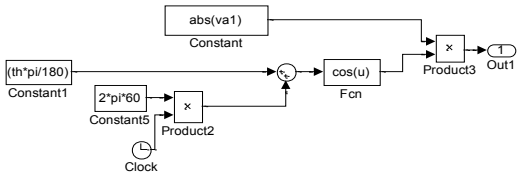

Fig. 3. Subsystem (Va_before_sag) Simulink model.

- Stator and rotor voltage equations

$$v_{qs} = \frac{p}{\omega_b}\psi_{qs} + r_s i_{qs} \quad , \quad v'_{qr} = \frac{p}{\omega_b}\psi'_{qr} - \frac{\omega_{re}}{\omega_b}\psi'_{dr} + r'_r i'_{qr}$$

$$v_{ds} = \frac{p}{\omega_b}\psi_{ds} + r_s i_{ds} \quad , \quad v'_{dr} = \frac{p}{\omega_b}\psi'_{dr} + \frac{\omega_{re}}{\omega_b}\psi'_{qr} + r'_r i'_{dr} \qquad (3)$$

$$v_{0s} = \frac{p}{\omega_b}\psi_{0s} + r_s i_{0s} \quad , \quad v'_{0r} = \frac{p}{\omega_b}\psi'_{0r} + r'_r i'_{0r}$$

- Flux linkage equations in matrix form

$$\begin{bmatrix}\psi_{qs}\\ \psi_{ds}\\ \psi_{0s}\\ \psi'_{qr}\\ \psi'_{dr}\\ \psi'_{0r}\end{bmatrix} = \begin{bmatrix} x_{ls}+x_m & 0 & 0 & x_m & 0 & 0\\ 0 & x_{ls}+x_m & 0 & 0 & x_m & 0\\ 0 & 0 & x_{ls} & 0 & 0 & 0\\ x_m & 0 & 0 & x'_{lr}+x_m & 0 & 0\\ 0 & x_m & 0 & 0 & x'_{lr}+x_m & 0\\ 0 & 0 & 0 & 0 & 0 & x'_{lr}\end{bmatrix}\begin{bmatrix} i_{qs}\\ i_{ds}\\ i_{rs}\\ i'_{qr}\\ i'_{dr}\\ i'_{0r}\end{bmatrix} \qquad (4)$$

- Torque equation

$$T_{em} = \frac{3}{2}\frac{P}{2\omega_b}(\psi_{ds} i_{qs} - \psi_{qs} i_{ds}) \quad \text{N.m.} \qquad (5)$$

For the sake of simulation in MATLAB/SIMULINK the q-axis of the stationary qd0 is taken always aligned with the stator a-phase and the motor is singly excited which means that, the rotor circuit is short circuited.

The torque equation given by (5) is the electromagnetic torque; the equation of motion of the rotor is obtained by equating the inertia torque to the accelerating torque as in (6),

$$J\frac{d\omega_r}{dt} = T_{em} - T_{mech} - T_{damp} \quad \text{N.m.} \qquad (6)$$

In equation (6), T_{mech} is the externally-applied mechanical torque in the opposite direction of rotor rotation (i.e., motoring action, for generating T_{mech} will be negative), T_{damp} is the damping torque in the opposite direction of rotor rotation and J is the rotor inertia.

When using (6) in conjunction with (3), the per unit (pu) speed (ω_{re}/ω_b), will be needed for building the speed voltage terms in the rotor voltage equations, thus (6) in terms of (ω_{re}/ω_b) yields to,

$$\frac{d(\omega_{re}/\omega_b)}{dt} = \frac{P}{2J\omega_b}(T_{em} - T_{mech} - T_{damp}) \quad \text{N.m.} \qquad (7)$$

Using these foregoing equations will help to build the three phase induction motor Simulink model shown in Fig. 4.

IV. SIMULATION DETAILS AND RESULTS

The methodology involved is as follows, the voltage sag generator will generate a three-phase balanced voltages to feed the IM at rated voltage and frequency, thus the motor is started normally and at certain time (sag initial time t_i) the voltage sag generator will apply a certain type of sags to the motor terminals for certain time (sag duration time Δt) with certain initial point-on-wave ψ_i, and certain magnitude h, then at the end of sag duration the voltage sag generator will re-apply the normal supply rated conditions to the motor terminals.

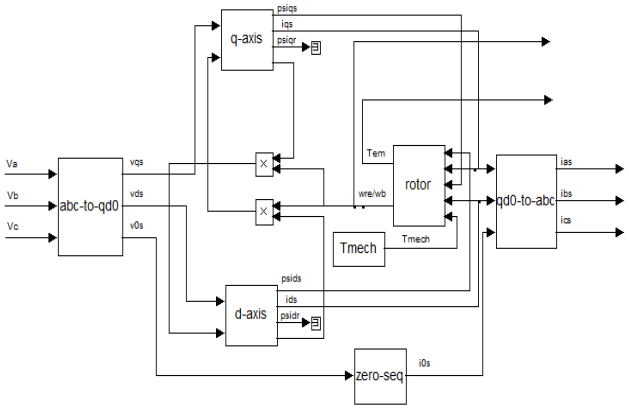

Fig. 4. Three phase IM Simulink model

TABLE II
PARAMETERS OF THE MOTORS USED IN ALL SIMULATIONS.

Motor HP rating	$r_s(\Omega)$	$r_r^{'}(\Omega)$	$L_s(H)$, $L_r^{'}(H)$	$L_m(H)$	$J(kg.m^2)$	$N_r(rpm)$
5	1.11500	1.08300	0.005974	0.20370	0.02	1750
10	0.68370	0.45100	0.004152	0.14860	0.05	1760
20	0.27610	0.16450	0.002191	0.07614	0.1	1760
50	0.09961	0.05837	0.000867	0.03039	0.4	1780
100	0.03957	0.02215	0.000389	0.01664	1.3	1780
150	0.03020	0.01721	0.000283	0.01095	2	1785

The effects of different voltage sags will be studied over six different motor sizes, where all these motors having ungrounded star connected stator, rated line voltage of 460 V, rated frequency of 60 Hz, lagging power factor of 0.75 and four poles. The parameters of each motor are given in table II (*N.B. the parameters of all motors are extracted from MATLAB/SIMULINK simpower systems library*).

To compare between different cases, the obtained simulation curves of stator currents, motor speed and torque are tabulated in per unit value with respect to each motor basis. The mechanical load (T_{mech}) is assumed to be of constant type with value of 0.6 of each motor rated output torque.

Since all motors have a star ungrounded stator, thus sags of type E and G of the same magnitude (h) and duration (Δt) have identical consequences since they have the same positive- and negative-sequence voltages, they only differ in the zero-sequence voltage, therefore we will deal with sags of type E only [3].

Voltage sag magnitudes can vary from 0.1 up to 0.9 pu and the initial point-on-wave can vary from 0º up to 180º. But most voltage sags have a magnitude of around 0.8 and duration of four to ten cycles [9-11].

So, in this paper we will simulate each sag type influence on each motor size in the following manners:

- The selected sag magnitudes are 0.8, 0.5, and 0.1 pu, where the magnitude of 0.8 pu represents the most probable sag magnitude, while the magnitude of 0.5 pu represents an intermediate sag magnitude and the magnitude of 0.1 pu represents the worst case sag magnitude.
- The selected initial point-on-wave values are 0º and 90º, these angles represent the extreme cases where the voltage function of time is assumed to be cosine wave.
- The selected sag durations are four and ten cycles.
- At each simulation, for certain motor HP rating and certain sag characteristics, the per unit peak current and peak torque are obtained during- and after-sag, while the lowest speed point during sag is obtained. Then all results are tabulated in per unit for each motor HP rating.
- All sag types (A, B, C, D, E, F) are generated with magnitude of 0.8 pu, with initial point-on-wave of 0º and 90º, then the generated wave forms are to be applied to each motor terminals. This is done to compare the effects of initial point-on-wave on torque, current and speed.
- Sag types (A, B, C) are generated with initial point-on-wave of 0º, with magnitudes of 0.5 and 0.1 pu, then the generated wave forms are to be applied to motor terminals. This is done to compare the effects of changing the sag magnitude on the motor behaviour. The simulation is done for sags A, B, and C where these sags represent the three-phase, single line-to-ground and two-phase faults respectively.
- For sag type A the instant that the motor retained its normal operating condition is recorded for each motor to study the effect of motor size and sag duration on the time needed for the motor to recover its normal operating conditions.
- The simulation duration is assumed to be seven seconds, the sag initial time t_i is assumed to be at the fifth second from the simulation start time, and the sag duration Δt is either 0.167 seconds (ten cycles) or 0.067 seconds (four cycles) after t_i.
  Since the initial conditions are not changed when changing the duration from ten cycles to four cycles, so in such cases we will care about the after sag data for studying the effect of sag duration on motor behaviour.

Simulation curves like Fig. 5, Fig. 6 and Fig. 7 are obtained to show the stator currents, motor speed and torque variations against the time period of interest respectively, also some values are labelled on the obtained curves where the X-variable is the time and the Y-variable is the speed, or current, or torque according to the plotted variable against time, then all these values are tabulated in per unit for each motor size and each sag type. Since this process will generate a large number of tables, samples of these tables like table III, and IV are shown for illustration.

V. RESULTS INVESTIGATION

In the previous section the effects of the different sag types on the induction motor stator currents, electromagnetic-torque and mechanical speed have been simulated.

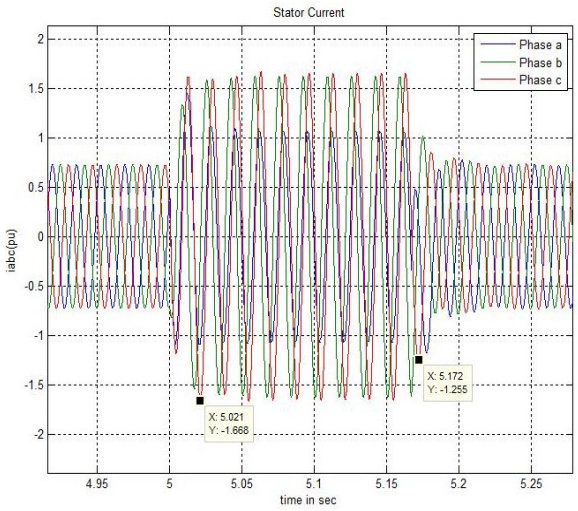

Fig. 5. A 5 HP Motor stator current for sag type B with, $h = 0.8$, $\psi_i = 0°$ and $\Delta t = 0.167$ seconds.

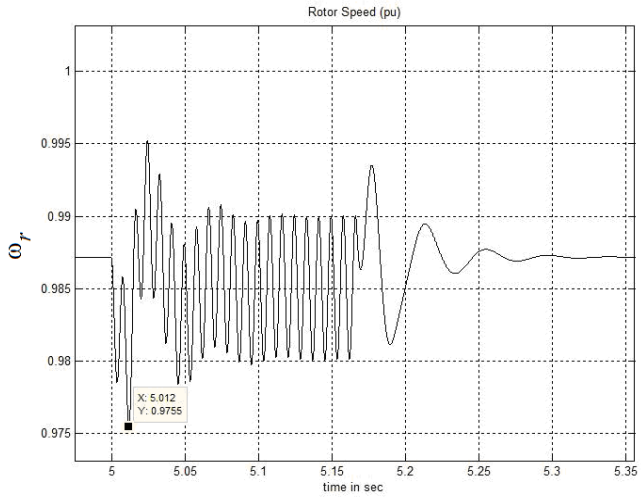

Fig. 6. A 5 HP Motor speed for sag type B with, $h = 0.8$, $\psi_i = 0°$ and $\Delta t = 0.167$ seconds.

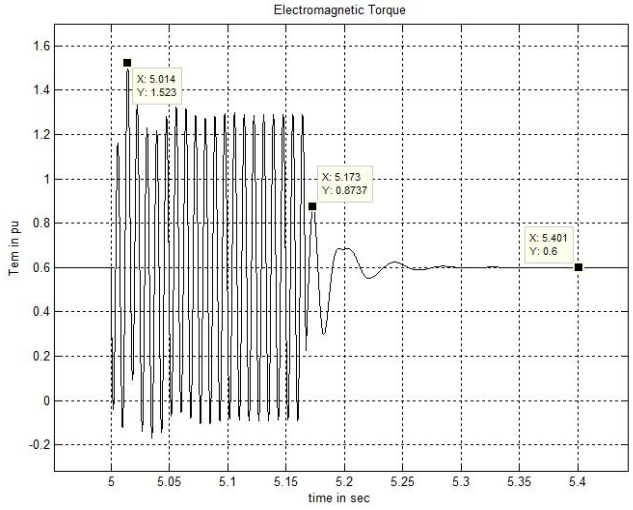

Fig. 7. A 5 HP Motor electromagnetic torque for sag type B with, $h = 0.8$, $\psi_i = 0°$ and $\Delta t = 0.167$ seconds

TAPLE III
Sag Type (A), with, $h = 0.8$, $\psi_i = 0°$ and $\Delta t = 0.167$ seconds.

Motor HP rating	During sag			After sag		Steady state time (seconds)
	Peak current (pu)	Peak torque (pu)	Lowest speed (pu)	Peak current (pu)	Peak torque (pu)	
5	1.936	1.874	0.9415	2.695	1.908	5.440
10	1.463	1.422	0.9578	2.217	1.684	5.586
20	1.563	1.542	0.9599	2.253	1.730	5.685
50	1.522	1.476	0.9720	2.262	1.730	5.708
100	1.788	1.584	0.9799	2.514	1.891	5.864
150	1.591	1.436	0.9807	2.350	1.831	5.904

TAPLE IV
Sag Type (A), with, $h = 0.1$, $\psi_i = 0°$ and $\Delta t = 0.167$ seconds

Motor HP rating	During sag			After sag	
	Peak current (pu)	Peak torque (pu)	Lowest speed (pu)	Peak Current (pu)	Peak Torque (pu)
5	8.178	0.006	0.1496	10.440	6.011
10	6.874	0.674	0.4050	8.200	2.769
20	7.276	1.312	0.4157	8.358	2.397
50	7.662	1.732	0.6470	8.466	3.259
100	8.992	2.423	0.7825	9.843	3.875
150	8.081	2.075	0.7919	8.824	3.666

The influence of the sag magnitude, the influence of initial point-on-wave and the sag duration have been simulated. All these simulations are done for six motor ratings of 5, 10, 20, 50, 100 and 150 HP. The restoration times for ten and four cycles type A sag have been recorded for all motor ratings.

The results have been obtained as curves using MATLAB/SIMULINK, and all data were tabulated as per unit quantities to compare between cases. The effects of the different sag types have been compared and the following notes can be obtained:

- If the sag is symmetrical, type A, the initial point-on-wave has little influence on the current peaks and almost no influence on the torque peaks or the speed variation. However, this point-on-wave has a great influence on the current and torque peaks when the fault is unsymmetrical, and little influence on the speed variation.
- It can be observed that the maximum current peaks for sags types B, D, and F are obtained when the initial point-on-wave is 90° [$v_a(t)$ is null and decreasing]. However, the maximum peaks are obtained in sags types C and E when the initial point -on-wave is 0° [$v_a(t)$ is maximum]. The same behaviour is seen in the torque peaks.
- The current and torque peaks during- and after-sag comparison shows that sag type A current and torque peaks after-sag are clearly higher than current and torque peaks during-sag, while the case is reversed in sag type B. Other sag types current and torque peaks are either closer in value or have small difference.
- The stator currents during the symmetrical sags (type A sags) are balanced as shown in Fig. 8, hence there is no negative-sequence torque produced, so that torque and speed variations with time are smooth as

shown in Fig. 9 and Fig. 10. But the stator currents in the other sag types are not balanced during the sag as shown in Fig. 5 which yields to produce negative-sequence torque which is responsible for the appearance of the un-damped oscillations in the torque and speed wave forms as shown in Fig. 6 and Fig. 7.

- Sags types E and G produce the same effects on the induction motor because their positive- and negative-sequence voltages are identical; this holds true for ungrounded star connected or delta connected IM.
- The drop in the motor speed is sever in case of sag type A and the severity increases as the sag magnitude decreases (i.e., h = 0.1 sag has larger speed drop than h = 0.8 sag), while sag type B has the least sever speed drop.
- The motor will recover its normal operating conditions in case of four cycles sag faster than the ten cycles sag. Moreover the smaller the motor size, the sooner it recovers its normal operating conditions.
- Low inertia motors are rapidly decelerate, which may lead to lose the continuity of the output, while high inertia motors undergo a limited amount of retardation and may be able to re-accelerate on voltage recovery.
- Depending upon the initial speed loss and the magnitude of the recovery voltage after fault clearing, the motors may accelerate taking a current depending upon their speed and starting characteristics. These currents may approach the starting currents of the motors, these acceleration currents flow through the supply system impedance, may prevent a fast recovery of system voltage (i.e., prolonging the sag event). The stronger the electrical system, in relation to the size of the accelerating motor, the greater the power available for the motor to accelerate and recover.
- On occurrence of voltage sag, an IM may stall and may not be able to accelerate its load on the restoration of the supply voltage to normal condition. To illustrate such case Fig. 11 and Fig. 12 show the torque and speed variations with time respectively for type A sag effect on the 5 HP motor with magnitude h = 0.1 pu, initial point-on-wave ψ_i = 0° and sag duration of Δt = 0.167 seconds. The figures show that the motor restored its normal operating conditions after sag, this could be explained as follows, the value of T_{mech} is selected to be smaller than the motor starting torque in this simulation, now, suppose this motor is loaded to a load which is larger than the motor starting torque, and after the motor reaches its steady state conditions a voltage sag event occurs, the motor behaviour during the sag event will be similar to that shown in Fig. 11 and Fig. 12, but after sag the motor will not be able to regain its normal conditions and hence stalling occurs.

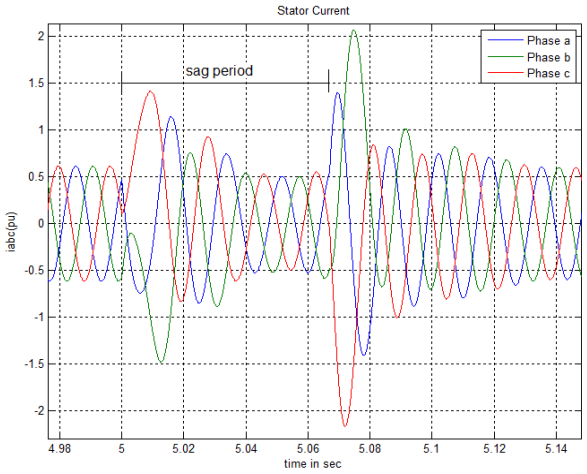

Fig. 8. A 10 HP Motor stator current for sag type A with, h = 0.8, ψ_i = 0° and Δt = 0.067 seconds.

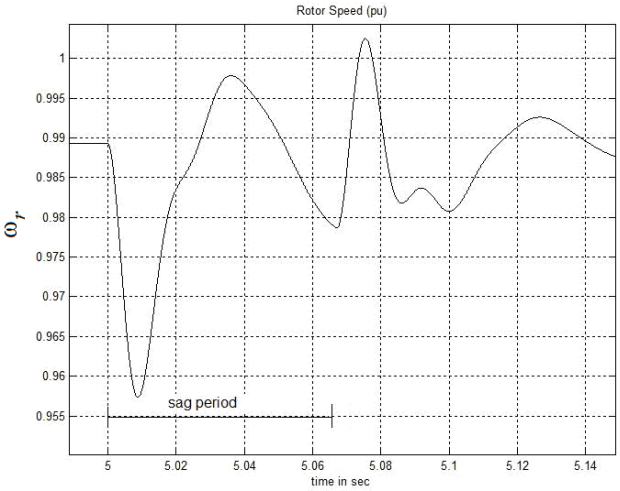

Fig. 9. A 10 HP Motor speed for sag type A with, h = 0.8, ψ_i = 0° and Δt = 0.067 seconds.

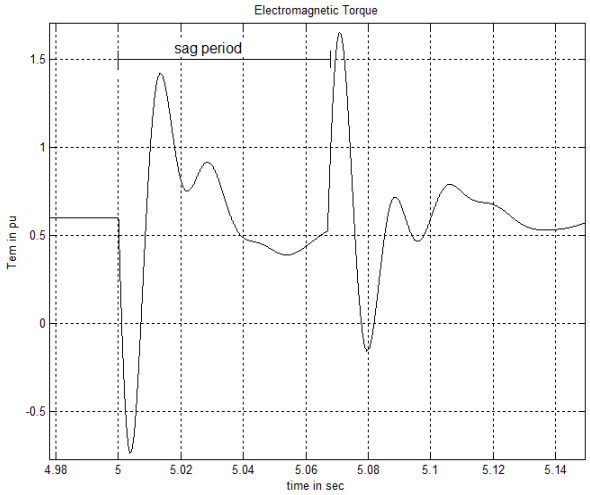

Fig. 10. A 10 HP Motor electromagnetic torque for sag type A with, h = 0.8, ψ_i = 0° and Δt = 0.067 seconds.

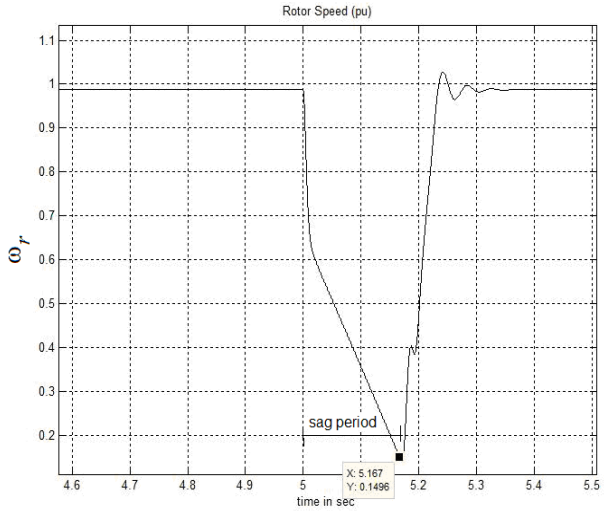

Fig. 11. A 5 HP Motor speed for sag type A with, $h = 0.1$, $\psi_i = 0°$ and $\Delta t = 0.167$ seconds

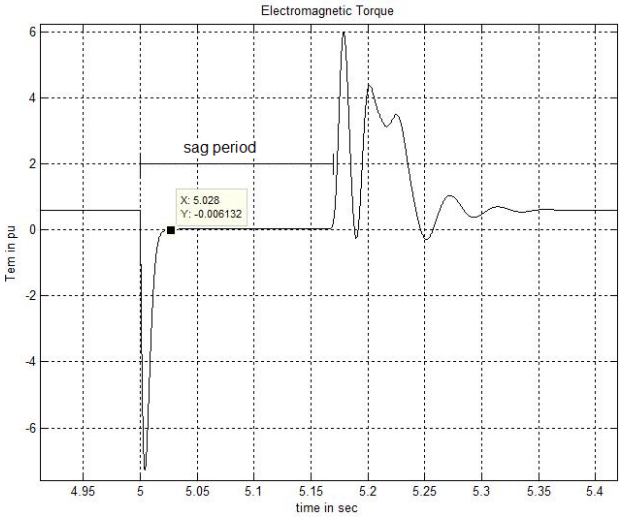

Fig. 12. A 5 HP Motor electromagnetic torque for sag type A with, $h = 0.1$, $\psi_i = 0°$ and $\Delta t = 0.167$ seconds.

VI. Conclusion

This paper presents a study to voltage sag influence on the three-phase induction motors where the three-phase induction motors, indeed, are the workhorses of today's industry, for the sake of this task an assessment of the performance of three-phase induction motors of different sizes when subjected to voltage sag of different types was carried out by building an induction motor transient model and a voltage sag generator model using MATLAB/SIMULINK package.

A survey was made to find out the most frequently occurred sag magnitudes and sag durations. Using the extreme point-on-wave angles and the commonly occurred sag magnitudes and durations several runs to the simulation model were done to obtain and tabulate the peak torque and peak current during and after sag as well as the lowest speed during sag as per unit quantities.

Investigations of the obtained results show that the induction motor was influenced by the sag magnitude, the sag duration, as well as the sag point-on-wave and this influence can be varied in severity according to the size of the motor and the type of the sag. The effects of voltage sag on the induction motor depend on the initial point-on-wave in case of unsymmetrical sags but it has almost a small or negligible effect in case of symmetrical ones. Type A sag has the most severe effects. The larger the motor size the smaller speed loss occurred; while the deeper the sag magnitude the higher speed loss occurred.

References

[1]. M. H. J. Bollen, "Understanding Power Quality Problems: Voltage Sags and Interruptions", New York: IEEE Press, 2000.

[2]. Lindong Zhang and Math H.J. Bollen, "Characteristic of Voltage Dips (Sags) in Power Systems", IEEE Transactions on power delivery, Vol. 15, No.2 April 2000, pp 827-832.

[3]. Luis Guasch, Felipe Córcoles, and Joaquín Pedra, "Effects of Symmetrical and Unsymmetrical Voltage Sags on Induction Machines", IEEE transactions on power delivery, vol. 19, No. 2 April 2004, pp. 774-782.

[4]. M. H. J. Bollen, Irene Yu-hua, "Signal Processing of Power Quality Disturbances", New York: IEEE Press, 2006.

[5]. Joaquín Pedra, Luis Sáinz, Felipe Córcoles, and Luis Guasch, "Symmetrical and Unsymmetrical Voltage Sag Effects on Three-Phase Transformers", IEEE transactions on power delivery, vol. 20, No. 2 April 2005, pp. 1683–1691.

[6]. Chee.Mun.Ong.," Dynamic Simulation of Electric Machinery Using MATLAB/SIMULINK". Prentice-Hall, 1998.

[7]. F.Córcoles, and J.Pedra. "Algorithm for the Study of Voltage Sags on Induction Machines", IEEE transactions on Energy Conversion, vol.14, No.4 December 1999, pp. 959-968.

[8]. Luis Guasch, Felipe Córcoles, and Joaquín Pedra, "Effects of Unsymmetrical Voltage Sag types E, F and G on Induction Motors", in Proc. 9th Int. Conf. Harmonics Quality Power, vol III, Orlando, October 2000, pp.796-803.

[9]. Juan C. Gomez, Medhat M. Marcos, Claudio A. Reineri, and Gabriel N. Campetelli, "Behavior of Induction Motor Due to Voltage Sags and Short Interruptions". IEEE transactions on power delivery, vol. 17, No.2 April 2002, pp. 434-440.

[10]. Jovica V. Milanovic, Myo T. Aung, , and Sarat C. Vegunta , "The Influence of Induction Motors on Voltage Sag Propagation—Part I: Accounting for the Change in Sag Characteristics", IEEE transactions on power delivery, vol. 23, No. 2 April 2008, pp. 1063–1071.

[11]. Jovica V. Milanovic, Myo T. Aung, , and Sarat C. Vegunta , "The Influence of Induction Motors on Voltage Sag Propagation—Part II: Accounting for the Change in Sag Performance at LV Buses", IEEE transactions on power delivery, vol. 23, No. 2 April 2008, pp. 1072–1078.